HINST: A 2-D CODE FOR HIGH-n TAE STABILITY.

N. N. Gorelenkov *, C. Z. Cheng, and W. M. Tang

Princeton Plasma Physics Laboratory

P.O. Box 451, Princeton, NJ 08543-0451

(April 18, 1998)

ABSTRACT

A high-n stability code, HINST, has been developed to study the stability of TAE (Toroidicity induced Alfvén Eigenmodes) in large tokamaks such as ITER where the spectrum of unstable TAE modes is shifted toward medium to high-n modes. The code solves the 2-D eigenmode problem by expanding the eigenfunction in terms of basis functions. Based on the Fourier-ballooning formalism the eigenmode problem is reduced to a system of coupled 1-D equations, which is solved numerically by using the finite element method and a SPARSE matrix solver. The numerical method allows to include non-perturbatively non-ideal effects such as: full ion FLR, trapped electron collisional damping, etc. The 2D numerical results of TAE and Resonance TAE modes are compared with those from local ballooning calculations and global MHD NOVA code. The results show that for ITER-like plasma parameters, TAE and RTAE modes can be driven unstable by alpha particles for $n = 10 - 20$. The growth rate for the most unstable mode is within the range $\gamma/\omega_A \simeq 0.3 - 1.5\%$. The most unstable modes are localized near $r/a \simeq 0.5$ and have a broad radial mode envelope width.

---

* *Permanent affiliation*: TRINITI, Troitsk, Russia 142092

I. INTRODUCTION

It is now generally acknowledged that Toroidal Alfvèn Eigenmodes [1–3] (TAE) destabilized by fast ions could cause significant difficulties for fusion ignition devices because of their capacity to induce large losses of fast particles. Even though TAE may play some positive role in burning tokamak-reactor plasma by means of providing a channel for fusion energy transfer to the plasma ions and He ash removal, the main concern here is that TAE induced losses could not only quench the ignition but also could lead to significant damage to the first wall. Previous low- to medium-n TAE instability studies indicated that fast particle drive $\gamma/\omega \sim n\beta_h(\rho_h/L_h)$, where n is the toroidal mode number, ρ_h is the fast ion Larmor radius, L_h is the fast ion pressure profile scale length, β_h is the fast ion thermal to magnetic pressure ratio. The fast particle drive reaches a maximum near $nq\rho_h/r \simeq 1$ and decreases with increasing n for $nq\rho_h/r > 1$. On the other hand, the radiative damping rate of TAE due to core ion FLR effects increases with $k_\perp\rho_i$ [4,5], where $k_\perp$ is the perpendicular wavelength of TAE and ρ_i is the bulk ion Larmor radius calculated for ions with thermal velocity $v_T = \sqrt{2T/m}$. Thus, it is expected that in large scale fusion devices such as ITER, JT-60SU, etc., where $\rho_{h,i}/L_h \ll 1$, medium- to high-n TAE modes can be potentially unstable. It is therefore an urgent research need for the tokamak project with ITER size to study the medium- to high-n TAE mode stability, which requires global numerical calculations.

The standard approach to high-n instabilities in toroidal system is via a WKB-ballooning analysis. In the context of the ballooning formalism originally introduced in Ref. [6], the radial mode envelope width is assumed to be of order $1/\sqrt{n}$ which is relevant in the case of ballooning modes. However, radial mode widths for TAE modes and toroidal drift modes are typically not strongly dependent on n, but instead are governed by the plasma equilibrium. This characteristic has recently motivated [7–9] the extension of the 1-D ballooning analysis to a 2-D analysis, which was also employed in numerical calculations [10].

The physics requirements for successful TAE stability code development were discussed in Ref. [5]. First, the code should be able to treat non-ideal effects non-perturbatively. There

are indications that non-ideal effects such as full FLR effects and fast ion drive can strongly influence not only the growth rate but also the eigenfrequency, the eigenmode structure, and, as we will see, the existence of some TAE branches, like Resonant TAE (RTAE) [5] or Energetic Particle Modes (EPM) [11,12]. Such modes may be related to experimentally observed Beam Driven Eigenmodes (BAE) [13,14]. Thus, it is of great interest to retain these non-ideal effects non-perturbatively in the code. Secondly, the code should be able to reproduce many other TAE branches, like kinetic TAE (KTAE) and non-circularity induced TAE (NAE). Damping mechanisms including radiative, collisional and resonant damping on plasma species should be considered. Also, fast particle drive needs to be calculated with full FLR effects and finite radial drift orbit width effects. The equilibrium needs to be represented numerically for reasonable Alfvén continuum and gap structure.

In this work, a numerical framework, the HINST (high-n toroidal stability) code, based upon a 2-D Fourier-Ballooning formalism with the capability of retaining non-ideal effects non-perturbatively, is developed. In contrast to the WKB-ballooning approach where obtaining the global eigenfrequency requires a detailed and labor intensive calculation of local ballooning eigenfrequencies, the Fourier-Ballooning approach allows direct calculations of the eigenfrequencies. The perturbation analysis based on the Fourier-Ballooning representation was presented in Ref. [15] in application to the study of ballooning modes, and in Ref. [16] to the study of TAE, where many results of previous work [1,7,8,17,18] were recovered.

In Section II, the 2-D Fourier-Ballooning formalism is presented. In Section III, a numerical procedure is given. In Section IV, the 2-D eigenmode equation with retained non-ideal and FLR effects is derived. Results are shown in Section V. Finally, a summary and conclusions are given in Section VI.

II. FOURIER-BALLOONING FORMALISM

We introduce the Fourier-Ballooning formalism for perturbed quantities in tokamak plasmas through the following $\hat{F}\hat{B}$ transformation, first, to a ballooning variable ϑ

$$\phi(r,\theta,\zeta,t) = \hat{B}\hat{\Phi} \equiv e^{-i\omega t - in(\zeta - q\theta)} \sum_j \hat{\Phi}(\theta + 2\pi j, r) e^{2\pi i j n q}, \tag{1}$$

where ζ is the ignorable toroidal angle and ω is the mode frequency. With this ballooning representation $\hat{\Phi}$ is no longer periodic in ϑ, where $\vartheta = \theta + 2\pi j$, and should vanish as $|\vartheta| \to \infty$ so that ϕ is periodic in θ. Considering that the safety factor $q(r)$ is a monotonically increasing or decreasing function of r, the Fourier transformation in the radial variable $x = n[q(r) - q_0]$ ($q_0 = q(r_0)$ is evaluated at a reference location r_0, which is typically chosen at the location of most unstable local TAE solution) to a new variable η_k is given by

$$\hat{\Phi}(\vartheta, x) = \hat{F}(x, \eta_k)\Phi \equiv \int e^{-ix\eta_k} \Phi(\vartheta, \eta_k) d\eta_k. \tag{2}$$

In the $\hat{F}\hat{B}$ transformation (Eqs.(1) and (2)), fast spatial variation is represented by $e^{inq\vartheta}$, while the envelope in ϑ, η_k space is given by the function $\Phi(\vartheta, \eta_k)$. The envelope function should satisfy the boundary conditions:

$$\begin{aligned} \Phi(\vartheta + 2\pi, \eta_k + 2\pi) &= \Phi(\vartheta, \eta_k), \\ \Phi(\vartheta, \eta_k) \to 0, |\vartheta - \eta_k| &\to \infty. \end{aligned} \tag{3}$$

Differential operators are transformed as follows:

$$\begin{aligned} \frac{\partial}{\partial\zeta}\phi \to -in\hat{F}\hat{B}\Phi, \frac{\partial}{\partial\theta}\phi \to \hat{F}\hat{B}\left(inq + \frac{\partial}{\partial\vartheta}\right)\Phi, \\ \frac{\partial}{\partial\psi}\phi \to \hat{F}\hat{B}\left(\vartheta - \eta_k\right) inq'\Phi, \nabla_{\|}\phi \to \hat{F}\hat{B}\frac{1}{\mathcal{J}B}\frac{\partial}{\partial\vartheta}\Phi, \end{aligned} \tag{4}$$

where $\mathcal{J}$ is the Jacobian and B is the equilibrium magnetic field.

The eigenmode equation is in general in the form of an integro-differential equation:

$$D(\omega, x, \theta, \nabla_\perp, \nabla_{\|})\phi = 0. \tag{5}$$

Applying the $\hat{F}\hat{B}$ transformation to Eq.(5) we obtain:

$$\hat{F}(x, \eta_k) D(\omega, x, \eta, \eta_k, \partial_\eta)\Phi(\eta, \eta_k) = 0, \tag{6}$$

where $\eta = \vartheta - \eta_k$, $\partial_\eta = \partial/\partial\eta$. To solve Eq.(6) we extract the radial dependence from the operator D, expanding it near the mode localization point $x = 0$

$$D(\omega, x, \eta, \eta_k, \partial_\eta) \simeq \sum_{l=0}^{L} D_l(\omega, \eta, \eta_k, \partial_\eta) x^l, \tag{7}$$

where L is the truncation number. We can now apply the inverse Fourier transform $\hat{F}^{-1}(\eta_k', x)f = (2\pi)^{-1} \int e^{ix\eta_k'} f dx$ to Eq.(6), which results in a 2-D eigenmode equation in the (η, η_k) space

$$\sum_{l=0}^{L} (\partial_{\eta_k} - \partial_\eta)^l D_l(\omega, \eta, \eta_k, \partial_\eta)(-i)^l \Phi(\eta, \eta_k) = 0, \tag{8}$$

with the boundary conditions

$$\begin{aligned} &\Phi(\eta, \eta_k + 2\pi) = \Phi(\eta, \eta_k), \\ &\Phi(\eta, \eta_k) \to 0, |\eta| \to \infty. \end{aligned} \tag{9}$$

Note that for $L = 0$, Eq.(8) reduces to a local ballooning equation.

III. NUMERICAL PROCEDURE

To obtain the numerical solution of Eq.(8), we present the solution in terms of a set of basis functions $\{\varphi_{p,u}\}$:

$$\Phi(\eta, \eta_k) = \sum_{p,u} A_{p,u}(\eta_k) \varphi_{p,u}(\eta), \tag{10}$$

where p and u are integers, the amplitude function $A_{p,u}$ is periodic in η_k with a period of 2π. The set of basis functions $\{\varphi_{p,u}\}$ must be complete and they should individually be very close to the local solutions of the eigenmode equation to provide a better convergence with a small number of terms in Eq.(10). The behavior of local TAE solutions has been obtained in previous works [1,7,8,17,18] and shows $\varphi_{p,u}(\eta) \sim e^{(i\Omega_0 \eta - \chi|\eta|)}$ which has a "fast" variation in η and an exponentially decaying behavior at $|\eta| \to \infty$, where the local eigenfrequency $\Omega_0 \equiv \omega q R / V_A \simeq 1/2$, and $0 < \chi < \epsilon_0 = r_0/R$. We choose the basis functions as follows:

$$\varphi_{p,u}(\eta) = e^{i\lambda_p \eta - \chi_u |\eta|} \equiv e^{\lambda_{p,u}' \eta}, \tag{11}$$

where $\lambda'_{p,u} = i\lambda_p - \chi_u \mathrm{sign}\,\eta$, $\lambda_p = p\ Re\Omega_0$, p and u are integers, χ_u is a discrete set of numbers taken to be evenly in the range $\{\chi_{\min}, \chi_{\max}\}$. $\Omega_0, \chi_{\min}$, and $\chi_{\max}$ are to be chosen according to the 1-D solution of the local eigenmode equation, i.e., Eq.(8) with $L = 0$. Ω_0 is usually chosen to be an eigenvalue of the 1-D local solution at the radial location with maximum growth rate in order to give an optimized representation of the most unstable mode. $\chi_{\min}$ and $\chi_{\max}$ represent the asymptotic behavior of the local solution at small η and at $\eta \to \infty$, respectively. Such a behavior is obtained numerically. Typically for TAE modes, we know the solution in η and use $\chi_{\max} = \epsilon_0$.

Operating with $\int d\eta \varphi_{p',u'}$ on Eq.(8), and substituting the solution in the form of Eq.(10), we obtain a coupled set of 1-D equations for the periodic functions $A_{p,u}(\eta_k)$:

$$\sum_{l',p,u} d_{l'p'u'pu}(\eta_k) \frac{\partial^{l'}}{\partial(\eta_k)^{l'}} A_{p,u}(\eta_k) = 0. \tag{12}$$

One can show that coefficients $d_{l'p'u'pu}$ have the following form:

$$d_{l'p'u'pu}(\eta_k) = \sum_{l=l'}^{L} \int \varphi_{p',u'} \varphi_{p,u} \frac{l!}{l'!(l-l')!} i^{-l} (\partial_{\eta_k} - \partial_\eta)^{l-l'} D_l(\omega, \eta, \eta_k, \lambda'_{p,u}) d\eta. \tag{13}$$

The numerical procedure for solving Eq.(12) is based on the finite element method in η_k. Thus, the eigenvalue problem is reduced to a matrix equation with the eigenvalues and eigenfunctions determined by requiring that the determinant of the matrix vanishes. The exact form of the eigenmode operator D will be given in the next section.

IV. 2-D EIGENMODE EQUATION

A. Basic Equation

We consider an analytic $s - \alpha_p$ equilibrium, where $s = rq'/q$ is the magnetic shear, $\alpha_p = -\beta'_p q^2 R$, β_p is plasma pressure to magnetic field pressure ratio. The high-n TAE eigenmode equation to be analyzed was derived in Ref. [5] based on the gyrokinetic equation. Assuming that bulk plasma species have Maxwellian equilibrium distribution functions, the perturbed particle distributions were obtained by solving gyrokinetic equations including

full ion FLR effects. The eigenmode equation in a form similar to Eq. (6) (except that it is additionally inverse Fourier transformed by $\hat{F}^{-1}$) is

$$\hat{F}^{-1}\hat{F}\left[\frac{\partial}{\partial\eta}h\frac{\partial}{\partial\eta}+[1+2\hat{\epsilon}\cos(\eta+\eta_k)]\frac{\omega^2}{\omega_A^2}\left(1-\frac{\omega_{*i}}{\omega}\right)\frac{h}{(1-G_1)(1+b_i)}\right.$$
$$\left.+\left[\alpha_{pc}(1-G_1)^{-1}+G_2\right]\right]\Phi+\hat{F}^{-1}\delta D=0, \qquad (14)$$

where $h=h(\eta,\eta_k)=1+[s\eta-\alpha_p\sin(\eta+\eta_k)]^2$, $\hat{\epsilon}\simeq 2[r/R+\Delta'(r)]$, $\Delta(r)$ is the Shafranov shift, R is the major radius, $\omega_A=V_A/qR$, $V_A^2=B_0^2/4\pi n_i M_i$, $\omega_{*i}/\omega_A=qk_\theta\rho_i\beta_i^{1/2}/2\epsilon_n$, $\epsilon_n=L_{pi}/R$, L_{pi} is the thermal ion pressure gradient scale length, $b_i=b_{\theta i}h$, $b_{\theta i}=(k_\theta\rho_i)^2/2$, $k_\theta=nq/r$, $G_1=(q_iT_e/q_eT_i)b_i/(1+b_i)/(1-\sqrt{2\epsilon}+i\delta_1)$, $G_2=-(\omega q\sqrt{\beta_i}/\omega_A k_\theta\rho_i)(1-\sqrt{2\epsilon}+i\delta_2)G_1/(1-G_1)$ and $\delta_1=\delta_2/1.46=3.22\pi\sqrt{\nu/2\omega}/\left(\ln 8\sqrt{\epsilon\omega/\nu}\right)^{3/2}$, $\epsilon=r/R$, and ν is the electron collisional frequency.

In this model dissipation due to trapped electron collision combines with bulk ion FLR effect to provide a parallel electric field, which is responsible for the radiative damping of TAE-like modes. For typical tokamak parameters, we expect $\delta_2>\delta_1\geq 0.01$ for TAE modes. In Eq.(14), full bulk ion Larmor radius effects are included via the Padé approximation. The nonadiabatic particle contribution denoted as δD includes wave-particle resonances and full FLR effects of both hot particles and bulk ions and accounts for both the hot particle drive and the bulk ion Landau damping. Even though the non-ideal contribution is proportional to particle β, they can have significant effects on TAE stability and generate new type of TAE modes. In Ref. [5] the hot particle contribution were assumed to be mainly due to deeply trapped particles with a slowing-down distribution function. The resonance contribution from such a δD_h provides a hot particle drive which is inversely proportional to the toroidal mode number. However, as we will demonstrate in the solution of gyrokinetic equation, only the passing particle contribution may give the dependence $Im\ \delta D_h\propto n$ for $k_\perp\rho_h\leq 1$, which is important for the high-n mode stability analysis.

Following Ref. [5] we have

$$\delta D_j\simeq -\frac{4\pi q^2R^2\omega q_j}{k_\theta^2c^2}\int d^3v\omega_k J_0(\sqrt{2b_j}v_\perp/v_T)g_j, \qquad (15)$$

where g_j is the nonadiabatic perturbed particle distribution function, J_0 is the Bessel function of zero order, $\omega_k = \mathbf{B} \times \kappa \cdot \nabla S(v_\parallel^2 + v_\perp^2/2)/\omega_{cj}$ is the toroidal curvature drift frequency, κ is the magnetic field curvature, $S = n(q\theta - \phi)$ is the eikonal, q_j and ω_{cj} is the charge and the cyclotron frequency of species j, respectively.

B. Nonadiabatic particle contribution

To derive the expression for the nonadiabatic ion particle contribution to the eigenmode equation, we need the nonadiabatic perturbed distribution function, which is determined from the gyrokinetic equation in the low frequency limit ($\omega \ll \omega_c$) [19,20]. Neglecting the parallel electric field effects for ion species the gyrokinetic equation is given by [5]:

$$\frac{dg_j}{dt} = \left(\frac{\partial}{\partial t} + (\mathbf{v}_\parallel + \mathbf{v_d}) \cdot \nabla\right) g_j = \frac{iq_j}{M_j}\frac{\partial F_j}{\partial \mathcal{E}}\left(1 - \frac{\omega_{*j}}{\omega}\right)\omega_k J_0 \phi. \tag{16}$$

where $\mathbf{v_d}$ is the particle magnetic drift velocity, $F_j = F_j(\psi, \mathcal{E}, \mu)$ is the equilibrium particle distribution, $\mathcal{E} = v^2/2$ is the particle energy per particle mass, $\mu = v_\perp^2/2$ is the magnetic moment per particle mass, and $\omega_{*j} = \mathbf{B} \times \nabla S \cdot \nabla F_j/(B\omega_{cj}\partial F_j/\partial \mathcal{E})$. In terms of the basis functions introduced in Section III this equation has the solution to the lowest order in $1/n$:

$$\begin{aligned} g_j = -\frac{iq_j}{2M_j}\sum_{p,u}\int_{-\infty}^{t} dt' \frac{\partial F_j}{\partial \mathcal{E}}\left(1 - \frac{\omega_{*j}}{\omega}\right)\hat{F}A_{p,u}(\eta_k)\varphi_{p,u}(\eta')v_d k_\theta J_0 e^{-i\omega t' + iS(t')} \\ \times \left(e^{i\vartheta'}(i + s\eta') + e^{-i\vartheta'}(i - s\eta') + \frac{i}{2}\alpha_p(e^{i2\vartheta'} + e^{-i2\vartheta'} - 2)\right), \end{aligned} \tag{17}$$

where the integration is along the unperturbed orbit, $\vartheta' = \vartheta(t')$, $\eta' = \eta(t')$. The expression Eq.(17) should be treated separately for trapped and passing particles.

1. Trapped particle contribution

For trapped particles one can make use of the equality

$$\int_{-\infty}^{t} = \sum_{\nu=0,\infty}\int_{t-(\nu+1)\tau_b}^{t-\nu\tau_b}$$

where τ_b is the period of particle motion in the plasma cross section (see, for example, Ref. [21]). Then, Eq.(17) can be written in the following way

$$g_j = -\frac{iq_j}{2M_j} e^{-i\omega t + iS(t)} \sum_{p,u;\nu=0,\infty} e^{i(\omega-\bar{\omega}_D)(\nu+1)\tau_b} \int_{t-(\nu+1)\tau_b}^{t-\nu\tau_b} dt' e^{-i\int_{t-(\nu+1)\tau_b}^{t'}(\omega-\omega_{Dpu})dt''} \hat{F} A_{p,u}(\eta_k)\varphi_{p,u}(\eta)$$
$$\times \frac{\partial F_j}{\partial \mathcal{E}} \left(1 - \frac{\omega_{*j}}{\omega}\right) v_d k_\theta J_0 \left(e^{i\vartheta'}(i + s\eta') + e^{-i\vartheta'}(i - s\eta') + \frac{i}{2}\alpha_p (e^{i2\vartheta'} + e^{-i2\vartheta'} - 2) \right), \quad (18)$$

where $\omega_{Dpu} = \omega_D - i\lambda_{p,u} d\vartheta/dt$, $\omega_D = dS/dt$, and the bar means the orbit average. One can show that the integrand in the RHS of Eq.(18) is a periodic function of time, which allows us to perform the sum over ν:

$$g_j = -\frac{iq_j}{2M_j} \frac{e^{-i\omega t + iS(t)}}{e^{-i(\omega-\bar{\omega}_D)\tau_b} - 1} \sum_{p,u} \int_{t-\tau_b}^{t} dt' e^{-i\int_{t-\tau_b}^{t'}(\omega-\omega_{Dpu})dt''} \frac{\partial F_j}{\partial \mathcal{E}} \left(1 - \frac{\omega_{*j}}{\omega}\right) \hat{F} A_{p,u}(\eta_k)\varphi_{p,u}(\eta)$$
$$\times v_d k_\theta J_0 \left(e^{i\vartheta'}(i + s\eta') + e^{-i\vartheta'}(i - s\eta') + \frac{i}{2}\alpha_p (e^{i2\vartheta'} + e^{-i2\vartheta'} - 2) \right). \quad (19)$$

To proceed further, we assume that trapped particles lives mostly near the bounce points, and that the resonant denominator in Eq. (19) leaves the contribution for particles, which are near the resonance

$$\omega - \bar{\omega}_D - I\omega_b = 0, \quad (20)$$

where I is the bounce harmonic number and $\omega_b = 2\pi/\tau_b$. Then, after some algebra, we reduce Eq.(19) to the approximate form

$$g_j \simeq -\frac{q_j}{2M_j} \frac{e^{-i\omega t + iS(t)}}{\omega - \bar{\omega}_D} \sum_{p,u} \frac{\partial F_j}{\partial \mathcal{E}} \left(1 - \frac{\omega_{*j}}{\omega}\right) \hat{F} A_{p,u}(\eta_k)\varphi_{p,u}(\eta) v_d k_\theta J_0$$
$$\times e^{\lambda'_{p,u}(2\pi N - \vartheta)} \left[i(X_1 + X_{-1}) + s(2\pi N - \eta_k)(X_1 - X_{-1}) \right.$$
$$\left. + \frac{i}{2}\alpha_p (X_2 + X_{-2} - 2X_0) + is\theta_b \left\{ \sin[(\lambda_p + 1)\theta_b] - \sin[(\lambda_p - 1)\theta_b] \right\} \right], \quad (21)$$

where

$$X_l = \cos\left[(\lambda_{p,u} + l)\theta_b\right]. \quad (22)$$

Here θ_b is the poloidal angle of trapped particle bounce point, N is the nearest integer to the ratio $\vartheta/(2\pi)$, and we have averaged over the sign of the parallel trapped particle velocity.

Note that in the above expression there are no bounce harmonics, which one can show is a good approximation provided the above assumption that the particle lives mostly near its turning point is taken into account. Thus, from Eq.(15) we obtain the nonadiabatic particle contribution

$$\delta D_j = -\frac{\pi q^2 R^2 \omega q_j^2}{c^2 M_j} \int d^3v v_d^2 J_0^2 \frac{e^{-i\omega t + iS(t)}}{\omega - \bar{\omega}_D} \frac{\partial F_j}{\partial \mathcal{E}} \left(1 - \frac{\omega_{*j}}{\omega}\right) \sum_{p,u} \hat{F} A_{p,u}(\eta_k) \varphi_{p,u}(\eta) e^{\lambda'_{p,u}(2\pi N - \vartheta)} X,$$

$$X = \left[e^{i\vartheta}(i + s\eta) + e^{-i\vartheta}(i - s\eta) + \frac{i}{2}\alpha_p(e^{i2\vartheta} + e^{-i2\vartheta} - 2)\right] \Big[i(X_1 + X_{-1})$$

$$+ s(2\pi N - \eta_k)(X_1 - X_{-1}) + \frac{i}{2}\alpha_p(X_2 + X_{-2} - 2X_0) + is\theta_b \left\{\sin[(\lambda_p + 1)\theta_b] - \sin[(\lambda_p - 1)\theta_b]\right\}\Big]. \quad (23)$$

The integrand in Eq.(23) can be factorized into two functions, $f(v)$ and $f(\theta_b) \equiv X$, in the large aspect ratio approximation when trapped particles have mostly perpendicular velocity. Then, the velocity space integration is reduced to the following

$$\int d^3v f(\theta_b) f(v) = \int v^2 f(v) dv \frac{\sqrt{\epsilon}}{2} I(\vartheta) = \int v^2 f(v) dv \frac{\sqrt{\epsilon}}{2} \int_{\pi}^{\vartheta - 2\pi N} \frac{f(\theta_b) \sin\theta_b d\theta_b}{\sqrt{\cos\vartheta - \cos\theta_b}}. \quad (24)$$

The integral in ϑ can be evaluated approximately using the fact that TAE is well represented by the basis function with $\lambda_p \simeq 1/2$. Then we have

$$I(\vartheta) \simeq \sqrt{\cos\vartheta + 1} \left\{[i(1 - \alpha_p/2) - s(2\pi N - \eta_k)\mathrm{sign}\lambda_p]\frac{8}{5}\cos(\lambda_p\vartheta)\right.$$

$$\left. + is\frac{5}{3}(2 - \cos\vartheta)\right\} \left[e^{i\vartheta}(i + s\eta) + e^{-i\vartheta}(i - s\eta) + \frac{i}{2}\alpha_p(e^{i2\vartheta} + e^{-i2\vartheta} - 2)\right]. \quad (25)$$

The velocity integration can be done for a Maxwellian distribution function, which allows us to present the trapped particle contribution in the form

$$\delta D_j \simeq -\frac{\beta_j q^2 \sqrt{\epsilon}}{4\sqrt{\pi}} I_v e^{-i\omega t + iS(t)} \left(1 - \frac{\omega_{*j}}{\omega}\right) \sum_{p,u} \hat{F} A_{p,u}(\eta_k) \varphi_{p,u}(\eta) e^{\lambda'_{p,u}(2\pi N - \vartheta)} I(\vartheta),$$

$$I_v = \int \frac{e^{-v^2/v_T^2} J_0^2}{1 - \bar{\omega}_{DT} v^2/\omega v_T^2} \frac{v^6 dv}{v_T^7}, \quad (26)$$

where the subscript T is referred to the quantity evaluated at the thermal velocity v_T. The expression for the integral I_v can be found by making use of the equations

$$2\int dx x^n e^{-x^2} J_0(ax) J_0(bx) \simeq \frac{\Gamma((n+1)/2)}{(1 + ab/2)^{(n+1)/2}} e^{-(a-b)^2/4}, \quad (27)$$

where we have used the Padé approximation. Eq. (27) is valid for odd n, but gives a good estimate for even n as well [22]. Using Eq.(27) and matching the results of integrations for I_v for the two limits $\bar{\omega}_{DT}/\omega \ll 1$ and $\bar{\omega}_{DT}/\omega \gg 1$, we obtain the expression

$$I_v = \frac{\sqrt{\pi}}{(1+b_i)^{5/2}} \frac{\left(1-\frac{\bar{\omega}_{DT}}{\omega}\right)\left(\frac{3}{1+b_j}+\frac{\bar{\omega}_{DT}^2}{\omega^2}\right)}{\left(1+\frac{\bar{\omega}_{DT}^2}{\omega^2}\right)^2} - \frac{i\pi}{2}\Sigma\left(\frac{\omega}{\bar{\omega}_{DT}}\right)^{7/2} e^{-\omega/\bar{\omega}_{DT}} J_0^2, \tag{28}$$

where $\Sigma = 0, \pi, 2\pi$ if $Imm\omega <, =, > 0$, respectively.

2. Passing particle contribution

To simplify the derivation, we will use here the approximation of a large aspect ratio equilibrium, which implies for passing particles:

$$\frac{dv_\parallel}{dt} = 0, \Rightarrow \vartheta = v_\parallel t/qR. \tag{29}$$

The perturbed nonadiabatic distribution is obtained from Eq.(17)

$$g_j \simeq -\frac{iq_j}{2M_j}\sum_{p,u}\frac{\partial F_j}{\partial \mathcal{E}}\left(1-\frac{\omega_{*j}}{\omega}\right)\hat{F}A_{p,u}(\eta_k)v_d k_\theta \int_\infty^t dt' \varphi_{p,u}(\eta') J_0(\sqrt{2b_j'}v_\perp/v_T) e^{-it'\omega+iS'} y(\vartheta',\eta'), \tag{30}$$

where prime means that the corresponding variables should be taken at the moment t', and the notation used is $y(\vartheta,\eta) = e^{i\vartheta}(i+s\eta) + e^{-i\vartheta}(i-s\eta) - 2i\alpha_p \sin^2\vartheta$. To get the contribution of passing particles we will substitute Eq.(30) into Eq.(15):

$$\delta D_j = -\frac{i\pi q^2 \omega M_j}{B^2}\sum_{p,u}\int\int d^3v dt' e^{-i\omega t'+iS'}\left(1-\frac{\omega_{*j}}{\omega}\right)\hat{F}A_{p,u}(\eta_k)\varphi_{p,u}(\eta') \times\left(v_\parallel^2+\frac{v_\perp^2}{2}\right)^2\frac{\partial F_j}{\partial\mathcal{E}}J_0 J_0' y' y, \tag{31}$$

which can be integrated in $v_\perp$ using the Maxwellian distribution function and Eq.(27). The result is

$$\delta D_j = \frac{iq^2\omega\beta_j}{2\sqrt{\pi}}\sum_{p,u}\int\int d\bar{v}_\parallel dt' e^{-\bar{v}_\parallel^2} e^{-i\omega t'+iS'}\left(1-\frac{\omega_{*j}}{\omega}\right)\hat{F}A_{p,u}(\eta_k) \times\varphi_{p,u}(\eta') e^{-(\sqrt{h}-\sqrt{h'})^2 b_{\theta j}/2} y' y\left(\frac{\bar{v}_\parallel^4}{1+\sqrt{b_j b_j'}}+\frac{\bar{v}_\parallel^2}{(1+\sqrt{b_j b_j'})^2}+\frac{1}{2(1+\sqrt{b_j b_j'})^3}\right), \tag{32}$$

where $\bar{v}_{\|} = v_{\|}/v_T$. To perform the time integration we note, that the time variation of the integrand is restricted by the exponent $e^{-(\sqrt{h}-\sqrt{h'})^2 b_{\theta j}/2}$. For the sake of simplicity we neglect this exponent substituting infinite limit with one defined $\int_{-\infty} \to \int_{-t_0}$, where $t_0 = qR/\sqrt{b_j/2}sv_{\|}$. Also we are going to neglected all sideband contributions and assume $\alpha_p^2 \ll 1$. One can obtain after this

$$\delta D_j = \frac{\beta_j q^2}{2\sqrt{\pi}} \left(1 - \frac{\omega_{*j}}{\omega}\right) \sum_{p,u} \hat{F} A_{p,u}(\eta_k) \varphi_{p,u}(\eta) e^{-i\omega t + iS(t)} (1 + s^2\eta^2) I_v^{pas},$$

$$I_v^{pas} = \int d\bar{v}_{\|} e^{-\bar{v}_{\|}^2} \left(\frac{\bar{v}_{\|}^4}{1+b_j} + \frac{\bar{v}_{\|}^2}{(1+b_j)^2} + \frac{1}{2(1+b_j)^3}\right) \left(\frac{1 - e^{-it_0(\omega-\omega_{D+1})}}{1-\omega_{D+1}/\omega} + \frac{1 - e^{-it_0(\omega-\omega_{D-1})}}{1-\omega_{D-1}/\omega}\right), \quad (33)$$

where $i\omega_{Dl} = (il + \lambda_{p,u})v_{\|}/qR$. We calculate the real part of the integral I_v^{pas}, presenting it in the form: $\int_0^{\bar{v}_{\|r}} + \int_{\bar{v}_{\|r}}^{\infty}$, where $\bar{v}_{\|r} = qr\omega/v_T|\lambda_p + \hat{l}|$, with $\hat{l} = \pm 1$, is the resonant parallel velocity, and taking the integrals in the limit $\omega^2/\omega_{D+1}^2 \gg 1$ for the first integral and $\omega^2/\omega_{D+1}^2 \ll 1$ for the second one. We also keep the imaginary part only in the resonance term which as one can show produces the biggest contribution. The resulting expression can be shown numerically to give a good approximation for I_v^{pas}:

$$\begin{aligned}
I_v^{pas} &= ReI_v^{pas} - \sum_{\hat{l}=\pm 1} i\pi \Sigma \bar{v}_{\|r} e^{-\bar{v}_{\|r}^2} (1 - e^{\chi_u/s\sqrt{b_{\theta j}/2}}) \left(\frac{\bar{v}_{\|r}^4}{1+b_j} + \frac{\bar{v}_{\|r}^2}{(1+b_j)^2} + \frac{1}{2(1+b_j)^3}\right), \\
ReI_v^{pas} &= (1 - e^{\chi_u/s\sqrt{b_{\theta j}/2}}) \sum_{\hat{l}=\pm 1} \left(\frac{I_0}{2(1+b_j)^3} + \frac{I_2}{(1+b_j)^2} + \frac{I_4}{1+b_j}\right), \\
I_0 &= 2\sqrt{\pi}\left(\frac{1}{2} - \bar{v}_{\|r}^2\right) \ \mathrm{erf}(\bar{v}_{\|r}) - 2\sqrt{\pi}\bar{v}_{\|r}^2 - 2\bar{v}_{\|r} e^{-\bar{v}_{\|r}^2}, \\
I_2 &= \sqrt{\pi}\left(\frac{1}{2} + \bar{v}_{\|r}^2\right) \ \mathrm{erf}(\bar{v}_{\|r}) - \sqrt{\pi}\bar{v}_{\|r}^2 - \bar{v}_{\|r} e^{-\bar{v}_{\|r}^2}, \\
I_4 &= \frac{\sqrt{\pi}}{4}\left(3 + 2\bar{v}_{\|r}^2\right) \ \mathrm{erf}(\bar{v}_{\|r}) - \frac{\sqrt{\pi}}{2}\bar{v}_{\|r}^2 - \left(2\bar{v}_{\|r}^2 + \frac{3}{2}\right) e^{-\bar{v}_{\|r}^2}, \qquad (34)
\end{aligned}$$

where erf() is the error function. Since we need to establish the overlap between HINST and previous calculations, we have to present the nonadiabatic contribution in linear form with the respect to the perturbed quantities, while the forms derived above are linear in terms of the basis functions. Thus, when comparing HINST results with the local ballooning code calculations, we choose $\lambda_p = \Omega_0$ in the nonadiabatic contribution.

V. RESULTS

A. TAE solution: HINST versus NOVA

TAE modes with frequencies inside the toroidicity induced gap in the Alfvén continuum are routinely reproduced in low-n ideal MHD codes, such as NOVA [23]. In order to benchmark the HINST code results we compare the eigenmode solutions of an $n = 6$ TAE mode for a TFTR DT plasma equilibrium. For the $n = 6$ TAE mode in TFTR plasmas HINST code formulation may be marginally applicable for such a medium toroidal mode numbers. The equilibrium is calculated for a TFTR shot number #73268 at 3.41 sec using the plasma profiles from the TRANSP data analyzing code [25]. The plasma parameters are: $R_0 = 2.52\,m$, $a = .87\,m$, $B_0 = 5\,T$, $\beta_{pc}(0) = 5\%$, central plasma electron density $n(0) = 7.3 \times 10^{13} cm^{-3}$ and the $q(r)$ profile is shown in Fig.1 along with the radial eigenmode structure of the poloidal harmonics of the radial component of the plasma displacement $\xi_\psi = \xi \cdot \nabla\psi$ obtained by the NOVA code. The TAE mode frequency is $f = \omega/2\pi = 265 kHz$. The solution from the HINST code is in good agreement with the NOVA code result. The $n = 6$ TAE mode solution obtained by the HINST code is shown in Fig. 2. The TAE eigenfrequency computed by the HINST code is about 5% higher than the NOVA's value. The mode structure (the mode radial location and envelope width) from the HINST code is quite similar to the NOVA's solution, although corresponding structure of the poloidal harmonics may differs slightly. There are several reasons for the difference in the mode structure: (1) in the HINST code the equilibrium profiles are fitted with a polynomial that is truncated by keeping a finite number of terms in the expansion series Eq.(10); (2) the eigenmode equation, Eq.(14), is derived based on the high$-n$ mode assumption and $n = 6$ is relatively "low" enough so that plasma profile and geometric effects are not fully included; and (3) finite ion Larmor radius effect is included in the HINST code, but not in the ideal MHD NOVA code.

B. TAE and RTAE modes in ITER-like plasmas

Employing the HINST code we have also performed TAE and RTAE stability calculations for ITER plasma profiles and parameters similar to those used in Ref. [10]: $R_0 = 6.05\,m$, $a = 2.3\,m$, $B_0 = 5.7\,T$, $T_e = T_i = T = T_0(1 - r^2/a^2)$, $n_e = n_{e0}(1 - r^2/a^2)^{1/2}$, $n_{e0} = 1.5 \times 10^{14}\,cm^{-3}$, $q = 1 + 2r^2/a^2$, $\beta_\alpha \sim n^2T^2$, $\delta_1 = 0.1(T/T_0)^{-3/4}$, and $\delta_2 = 0.16(T/T_0)^{-3/4}$. We assume a DT plasma with an equal mixture and same density and temperature profiles as electrons.

First we consider TAE stability in a low plasma beta ITER plasma by setting the bulk particle temperature to be $T_0 = 10\,KeV$, the total core plasma beta at the magnetic axis is $\beta_{pc} = 3.7\%$ and $\beta_{\alpha 0} = 0.25\%$. For this plasma condition, TAEs exist inside the continuum gap and are destabilized by alpha particles. The most unstable $n = 10$ TAE mode has a real frequency $\omega_r/\omega_{A0} = 0.251$, where $\omega_{A0} = V_A(0)/q(0)R$, which agrees with Ref. [10] and is located inside the continuum gap near $r/a \simeq 0.5$ as shown in Fig. 3. The TAE growth rate is $\gamma/\omega_{A0} = 1\%$ which is different from the value given in Ref. [10] because of a different driving mechanism and full FLR effects included in the HINST code. Also shown in Fig. 3 are local TAE eigenfrequencies from the 1-D calculation (Eq.(8) with $L = 0$) at a fixed value of $\eta_k = 0$. Note that the local TAE growth rate is maximum near the radial location $r/a \simeq 0.5$. The corresponding 2D radial mode structures of poloidal harmonics with mode numbers $13 < m < 19$ are shown in Fig. 4, which clearly show that the TAE mode is localized near the maximum local growth rate location. The 2D calculation was performed with 20 basis functions ($-2 \le p \le 2$, $1 \le u \le 4$). The envelope function $A_{p,u}(\eta_k)$ for $p = 1, u = 1$ ($\lambda_p = 0.25p$, $\chi_1 = 0.005$, $\chi_4 = r_0/R$) computed by the HINST code, is shown in Fig. 5. The number of grid points in η_k is 30. One can see that the envelope function is localized near $\eta_k = 0$. Results show that the eigenfunction $\Phi(\eta, \eta_k = 0)$ agrees well with the local ballooning solution at $r/a = 0.5$. Therefore, we expect that this TAE mode can be studied reasonably well by means of a 2D WKB-ballooning formalism [10].

It was shown previously [5] that as the core plasma β increases the TAE mode can be

transformed into a resonant type TAE mode (RTAE) in presence of strong alpha particle drive. Thus, we increase the core ITER plasma temperature to $T_0 = 20\,KeV$, the total core plasma beta at the magnetic axis is $\beta_{pc}(0) = 7.4\%$ ($< \beta_{pc} >= 2.96\%$) and the most unstable eigenmode frequency shifts down into continuum. We identify the unstable mode as RTAE mode [5] which has $\omega/\omega_{A0} = 0.2$, $\gamma_r/\omega_{A0} = 0.0165$, and $11 < m < 19$ are the dominant poloidal harmonics and their radial mode structures are shown in Fig. 6. The mode is broad in r and shows a singular behavior which is typical for modes inside the continuum. The envelope function $A_{p,u}(\eta_k)$ for $p = 1, u = 1$ shown in Fig. 7 is is broader for RTAE than that for TAE mode. Thus, after inverse Fourier transform to the real space there are more poloidal harmonics to cover a broader radial domain. With $\delta_1 = \delta_2 = 0$ the RTAE growth rate is $\gamma/\omega_{A0} = 0.0185$ which is about 10% higher so that the effect of collisional radiative damping due to electrons is small.

However, because the RTAE is a non-perturbative solution it is strongly affected by the change in the fast particle drive (α_h). The RTAE mode is stabilized for $\beta_{h0} < \beta_{hcr} = 0.6\%$, which is slightly lower than the critical value, $\beta_{hcr} = 0.8\%$, of local calculations at $r/a = 0.6$ where the $m = 18$ harmonic amplitude is large. This is probably because alpha drive in the $r/a < 0.6$ region is larger and can contribute more to the stability of RTAE mode. Also, the ion Landau damping is usually small $\gamma_i/\omega_{A0} = 0.1\%$, which may be due to the use of the $s - \alpha$ equilibrium model that neglects the ellipticity effect. The ellipticity may lead to higher ion Landau damping because of the coupling through sideband resonances. We have also investigated the stability of KTAEs and found that they are usually stable because of high radiative damping effects.

VI. SUMMARY AND CONCLUSIONS

A high-n stability code, HINST, based on the Fourier-ballooning formalism has been developed and is shown to be able to study the stability of various types of TAEs in large tokamaks such as ITER where the spectrum of unstable TAEs is shifted toward medium to

high-n modes. The HINST code adopts a non-perturbative approach for calculating non-ideal effects such as: full ion FLR, trapped electron collisional damping, etc. The HINST code has been benchmarked successfully against local ballooning calculations and the global MHD NOVA code. It has been benchmarked carefully with both the global NOVA code as well as the high-n WKB-ballooning code.

We have studied TAE stability of ITER-like plasma parameters and the results show that for low core plasma β ($\beta(0) \simeq 4\%$) TAE modes with $n = 10 - 20$ are unstable. As $\beta(0)$ increases to 7.4% resonant type TAEs (RTAE) with frequencies inside the lower Alfvén continuum are driven unstable by alpha particles. The most unstable RTAE mode has $\gamma/\omega_A \simeq 1.6\%$ and is localized near $r/a \simeq 0.5$ with very broad radial structure.

The HINST code is still being improved in several areas: (1) the capability of handling non-circular plasma shaping effects, which are important in determining thermal ion Landau damping and fast particle drive; (2) the reformulation of fast ion response to allow for non-Maxwellian particle distributions such as the slowing-down distribution function; (3) improvement of some non-ideal effects such as trapped electron collision. Finally, a more complete comparison with other kinetic 2D codes such as the NOVA-K code is still to be carried out.

ACKNOWLEDGMENT

The authors would like to thank Drs. G. Y. Fu, G. Rewoldt, J. W. Van Dam, H. L. Berk and L. Chen for helpful discussions.
This work was supported by US DoE contract DE-AC02-76-CHO-3073.

---

[1] C. Z. Cheng, L. Chen, M. S. Chance, Ann Phys. (NY) **161**, 21 (1985).

[2] C. Z. Cheng and M. S. Chance, Phys. Fluids **29**, 3695 (1986).

[3] G. Y. Fu and J. W. Van Dam, Phys. Fluids B **1**, 1949 (1989).

[4] R. R. Mett and S. M. Mahajan, Phys. Fluids B **4**, 2885 (1992).

[5] C. Z. Cheng, N. N. Gorelenkov, and C. T. Hsu, Nucl. Fusion **35**, 1639 (1995).

[6] J. W. Connor, R. J. Hastie, and J. B. Taylor, Proc. R. Soc London Ser. A **365**, 1 (1979).

[7] F. Zonca, Ph.D. thesis, Princeton University, 1993.

[8] F. Zonca and L. Chen, Phys. Fluids B **5**, 3668 (1993).

[9] J. W. Connor, J. B. Taylor, and H. R. Wilson, Phys. Rev. Lett. **70**, 1803 (1993).

[10] G. Vlad, et al., Nucl. Fusion **35**, 1651 (1995).

[11] L. Chen, Phys. Plasmas **1**, 1519 (1994).

[12] R. A. Santoro and L. Chen, Phys. Plasmas **3**, 2349 (1996).

[13] W. W. Heidbrink, et al. Phys. Rev. Lett. **71** 855 (1993).

[14] W. W. Heidbrink, G. J. Sadler, Phys. Rev. Lett. **71** (1993) 855.

[15] Y. Z. Zhang and S. M. Mahajan, Phys. Lett. A **157**, 133 (1991).

[16] X. D. Zhang, Y. Z. Zhang, S. M. Mahajan, Phys. Fluid B **5**, 1257 (1993).

[17] M. N. Rosenbluth, et al. Phys. Rev. Lett. A **68**, 596 (1992).

[18] H. L. Berk, et al., Phys. Fluid B **4**, 1806 (1992).

[19] T. M. Antonsen and B. Lane, Phys. Fluids **23**, 1205 (1980).

[20] P. J. Catto, et al., Plasma Phys., **23**, 639 (1981).

[21] Mikhailovskii, A. B., in *Reviews of Plasma Physics*, edited by M. A. Leontovich (Consultants Bureau, New York, 1986), Vol. 9, p. 103.

[22] I. S. Gradshteyn and I. M. Ryzhik, *Table of Integrals, Series and Products.* Academic, San

Diego, Calif., 1963.

[23] C. Z. Cheng and M. S. Chance, J. Comput. Phys., **71**, 124-146 (1987).

[24] C. Z. Cheng, Phys. Reports, **211**, 1, (1992).

[25] R. V. Budny, Nucl. Fusion **34**, 1247 (1994)

FIGURES:

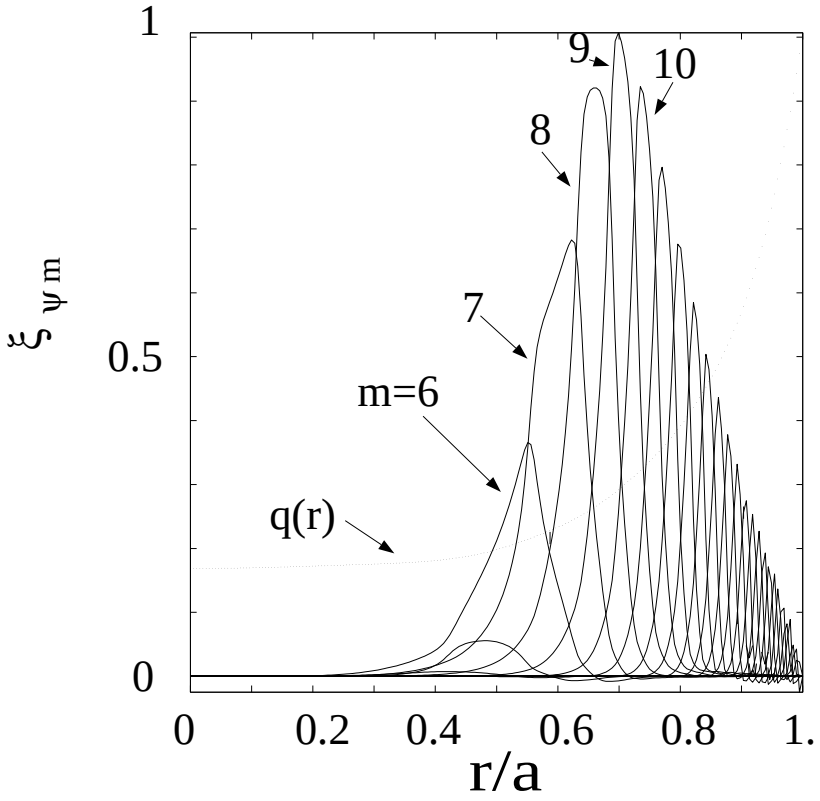

FIG. 1. Radial structure of poloidal harmonics of a $n = 6$ TAE mode radial displacement obtained by NOVA for TFTR plasma (shot # 73268 at 3.41 sec).

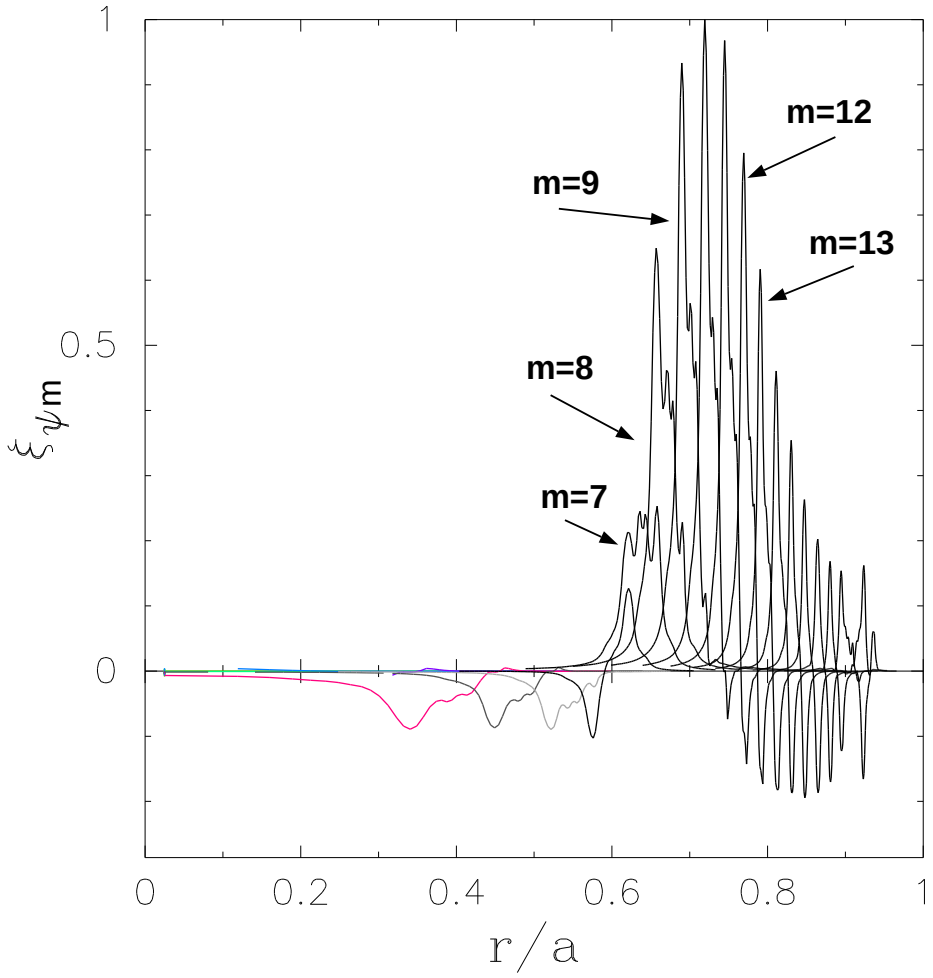

FIG. 2. TAE eigenmode radial structure obtained from HINST for the same TFTR plasma as in Fig.1.

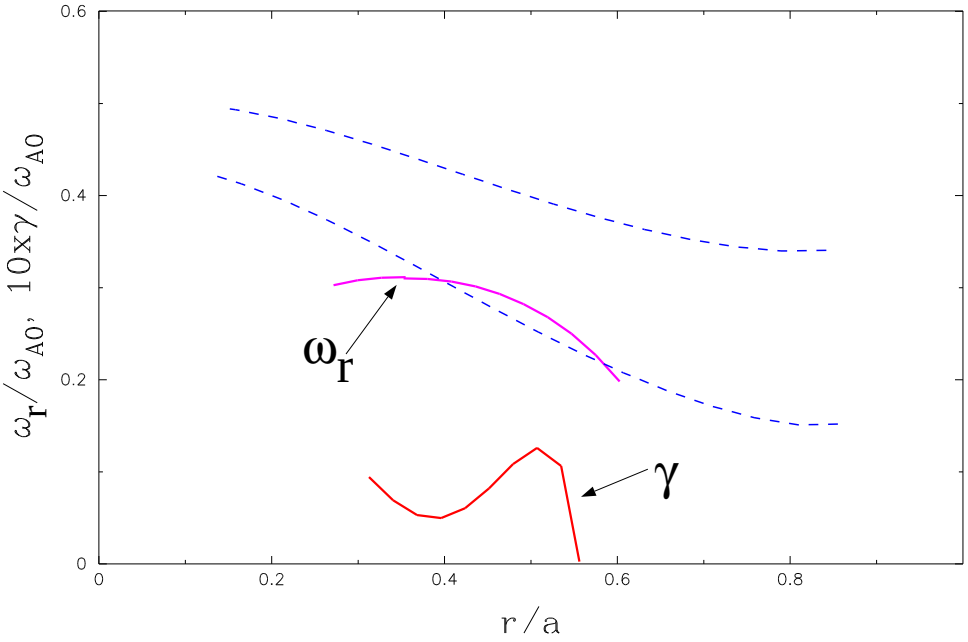

FIG. 3. Infinite-n gap structure and $1D$ local TAE eigenfrequency at fixed $\eta_k = 0$ for an ITER-like equilibrium with $\beta_{pc}(0) = 3.7\%$.

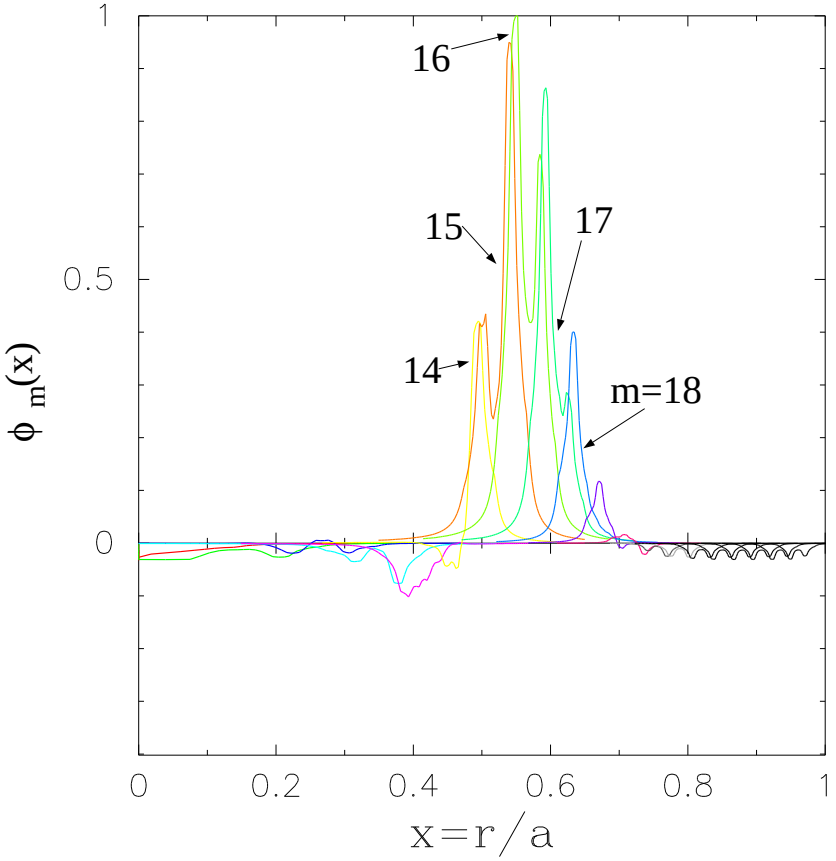

FIG. 4. The radial structure of poloidal harmonics of an $n = 10$ TAE mode.

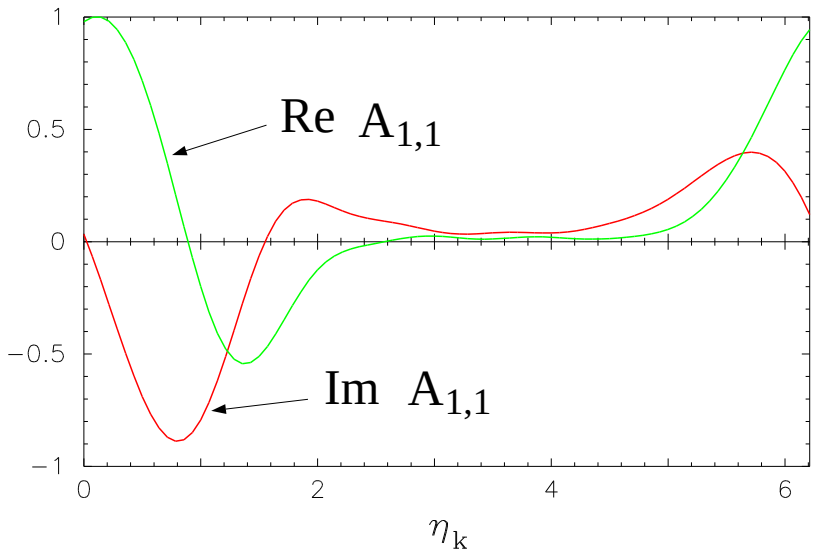

FIG. 5. Envelope function $A_{p,u}(\eta_k)$, defined in Eq.(10), for $p = 1$, $u = 1$ in radial Fourier variable η_k space for a global TAE mode.

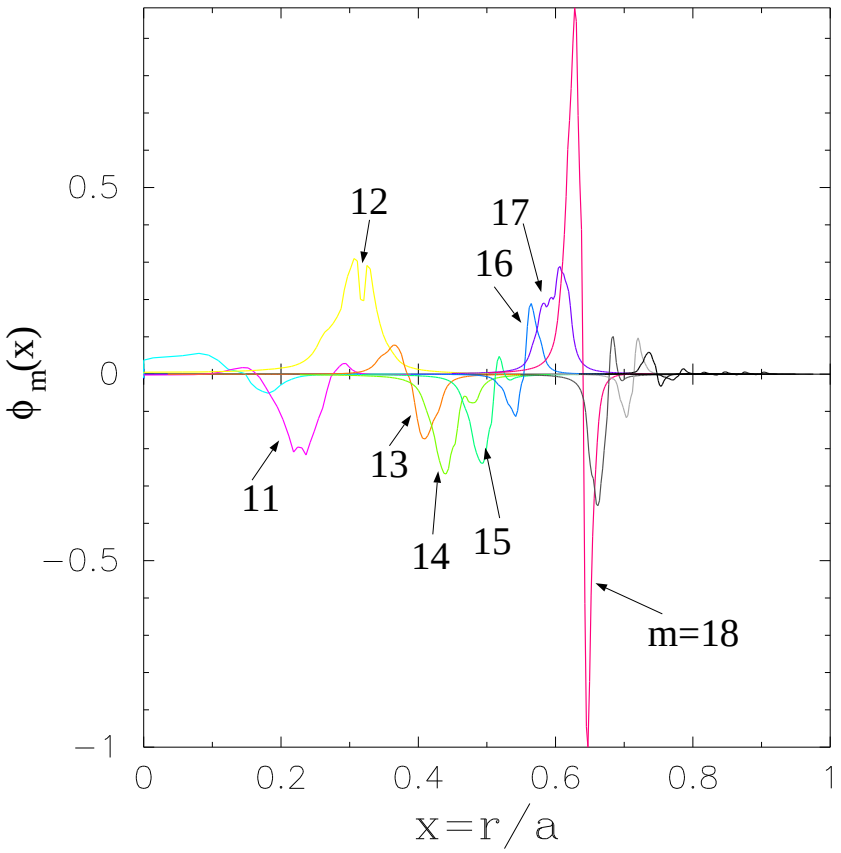

FIG. 6. The radial structure of poloidal harmonics of an $n = 10$ RTAE mode at $\beta_{pc} = 7.4\%$.

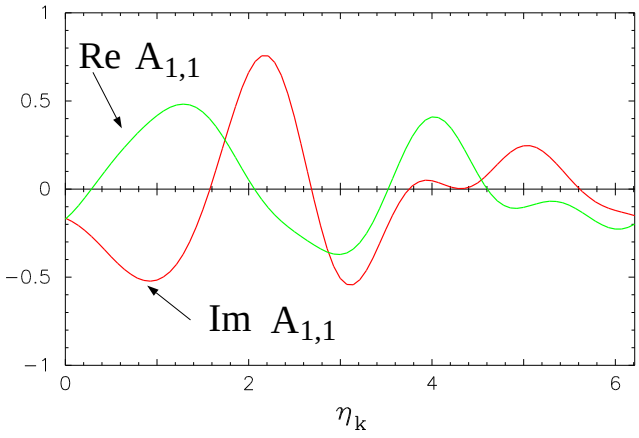

FIG. 7. Envelope function $A_{p,u}(\eta_k)$, defined in Eq.(10), for $p = 1$, $u = 1$ in radial Fourier variable η_k space for a global RTAE mode for $\beta_{pc} = 7.4\%$.